

Vacuum stability at cryogenic temperature

WP4 - Activity at LNF

Karlsruhe, 17/10/2018

Luisa Spallino, Marco Angelucci, Rosanna Larciprete
and Roberto Cimino



EuroCirCol Meeting in Karlsruhe

- **Summary of the main activities**
 - Dose calibration
 - Temperature calibration
 - Ar TPD measurements: data analysis and results
- **CH₄ and CO TPD measurements**

Vacuum stability at cryogenic temperature

LHC
Synchrotron Radiation
Power = 0.13 W/m

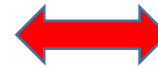
FCC
Synchrotron Radiation
Power = 40 W/m

Temperature/Pressure
Variation



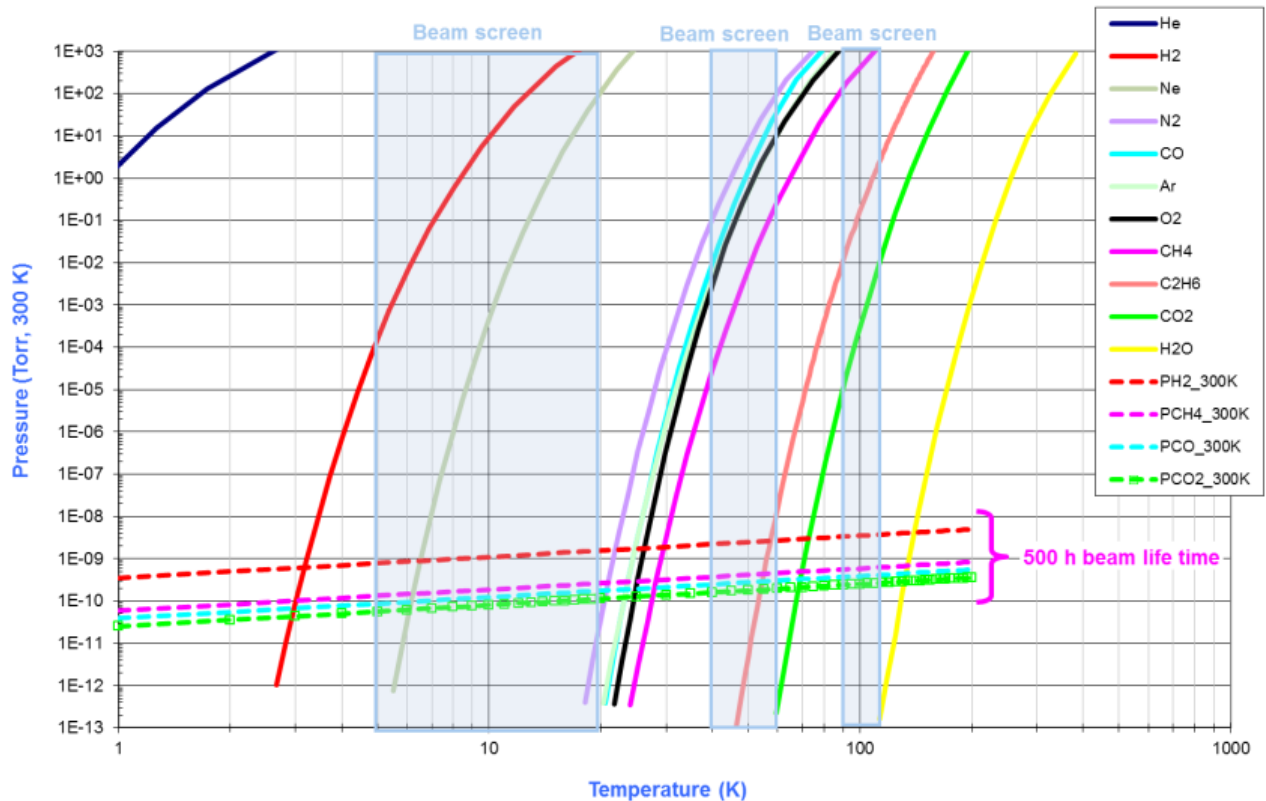
Beam life Time

Working Pressure
($<10^{-11}$ mbar)



Beam screen
Temperature Range

Saturated vapour pressure from Honig and Hook (1960) (C2H6 Thibault et al.)

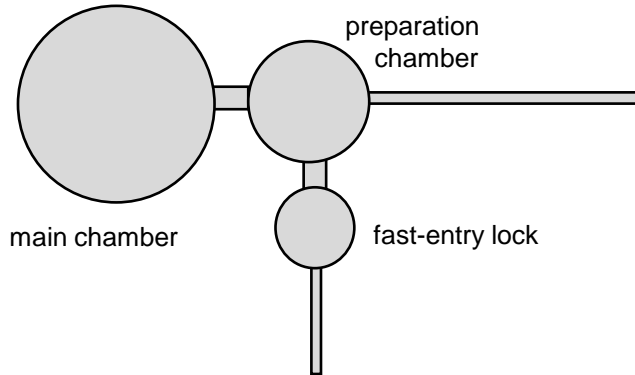


Independently on the substrate treatment, the vacuum stability due to the desorption of residual contaminant gases has to be guaranteed

Our task

Study of adsorption/desorption behaviour of typical contaminant gases in accelerators near their critical temperatures as a function of the surface morphology

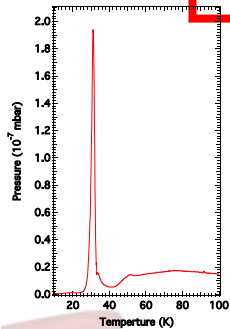
Ultra high vacuum systems



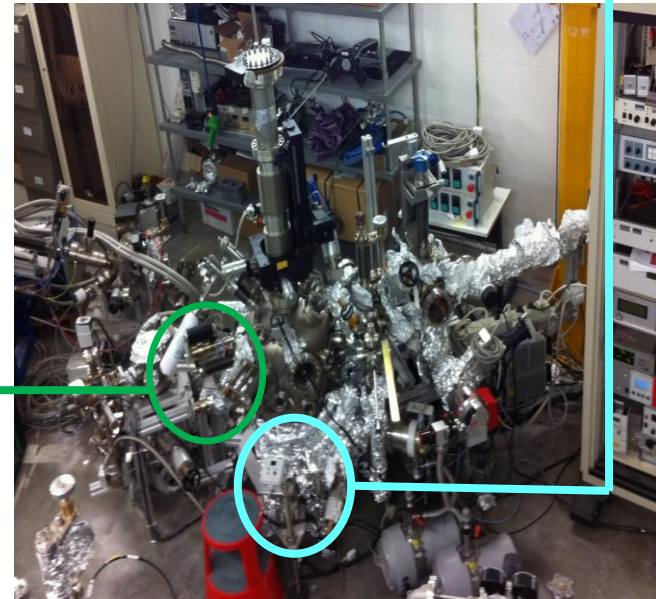
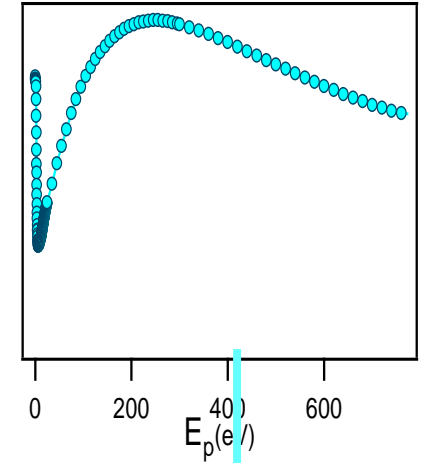
- LNF-cryogenic manipulator
- Sample at 15-300 K

Temperature Programmed
Desorption (**TPD**) measurements

Equipment : QMS (Hiden HAL 101 Pic)

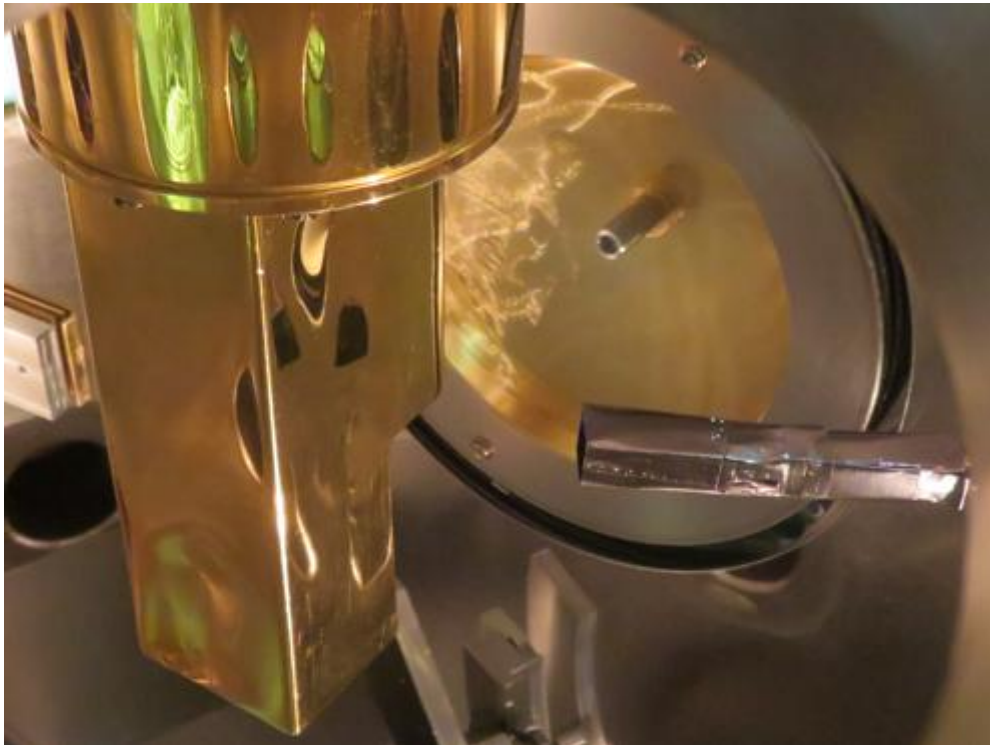


Secondary
Electron Yield
(**SEY**)
measurements
Equipment : Electron
gun, Faraday cup

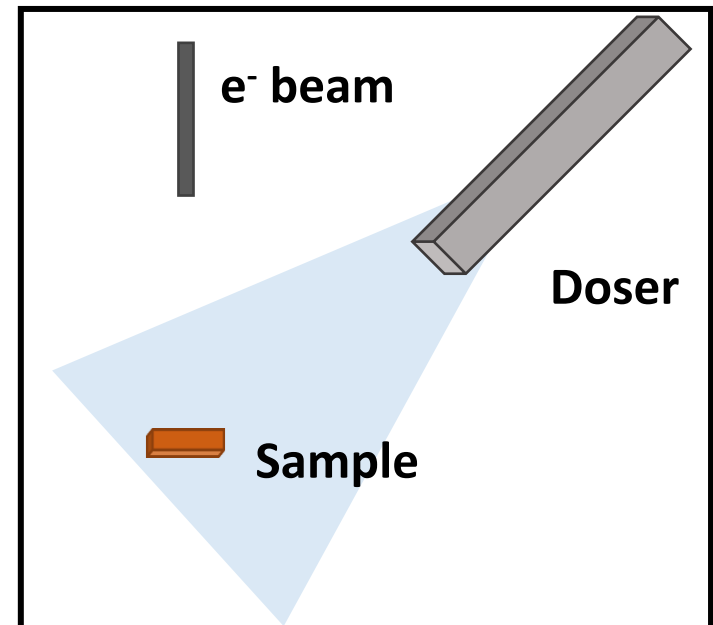


Dose calibration

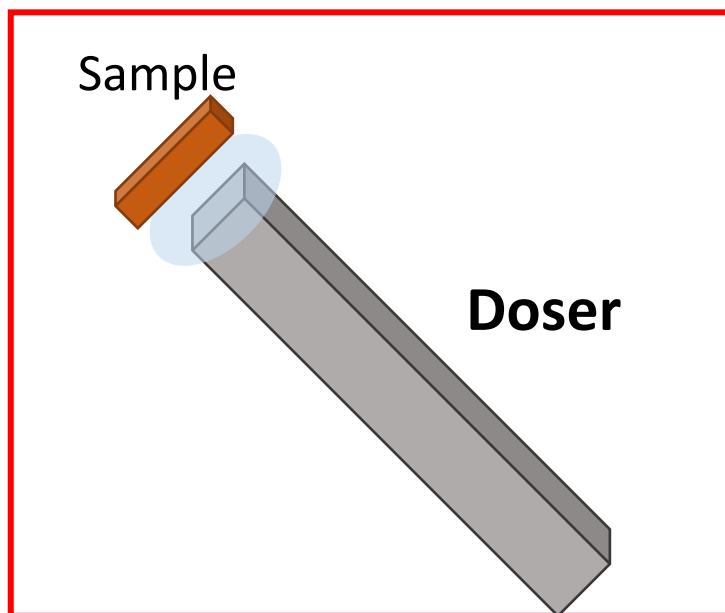
Gas dosing



Far from the sample



Near to the sample

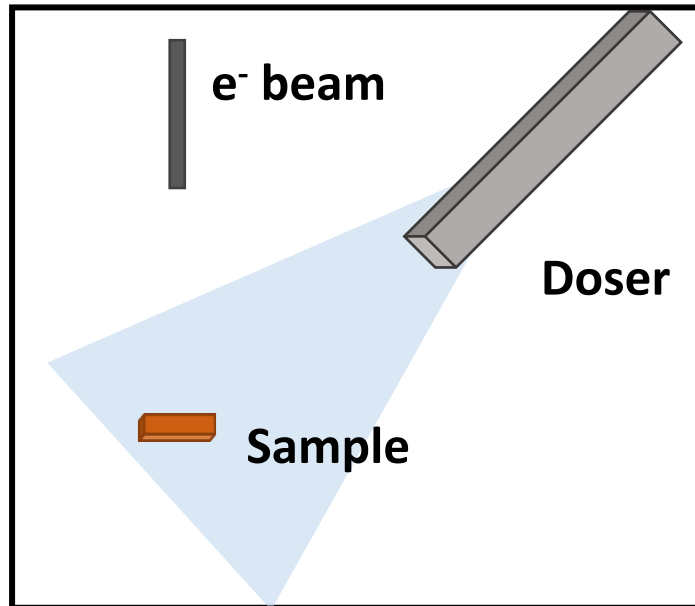


Dose calibration

Different local pressure on the sample

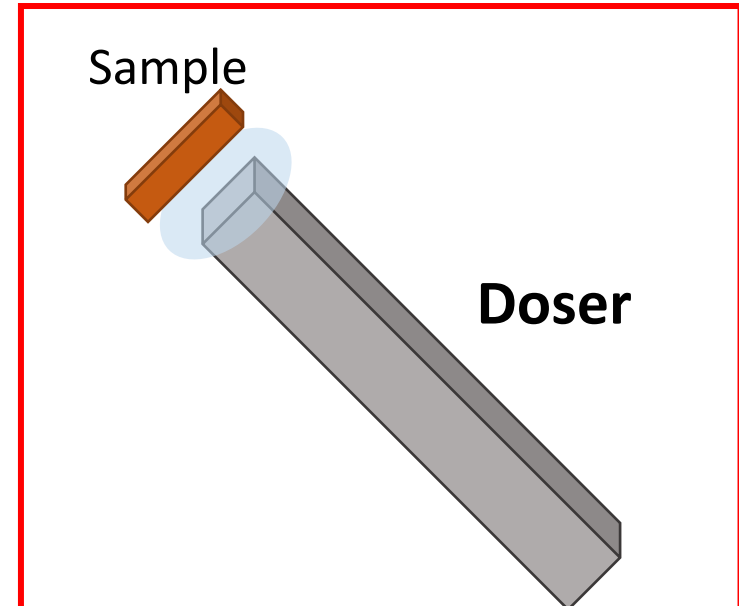
1s@ 1.33×10^{-6} mbar corresponds to

Far from the sample



1 Langmuir

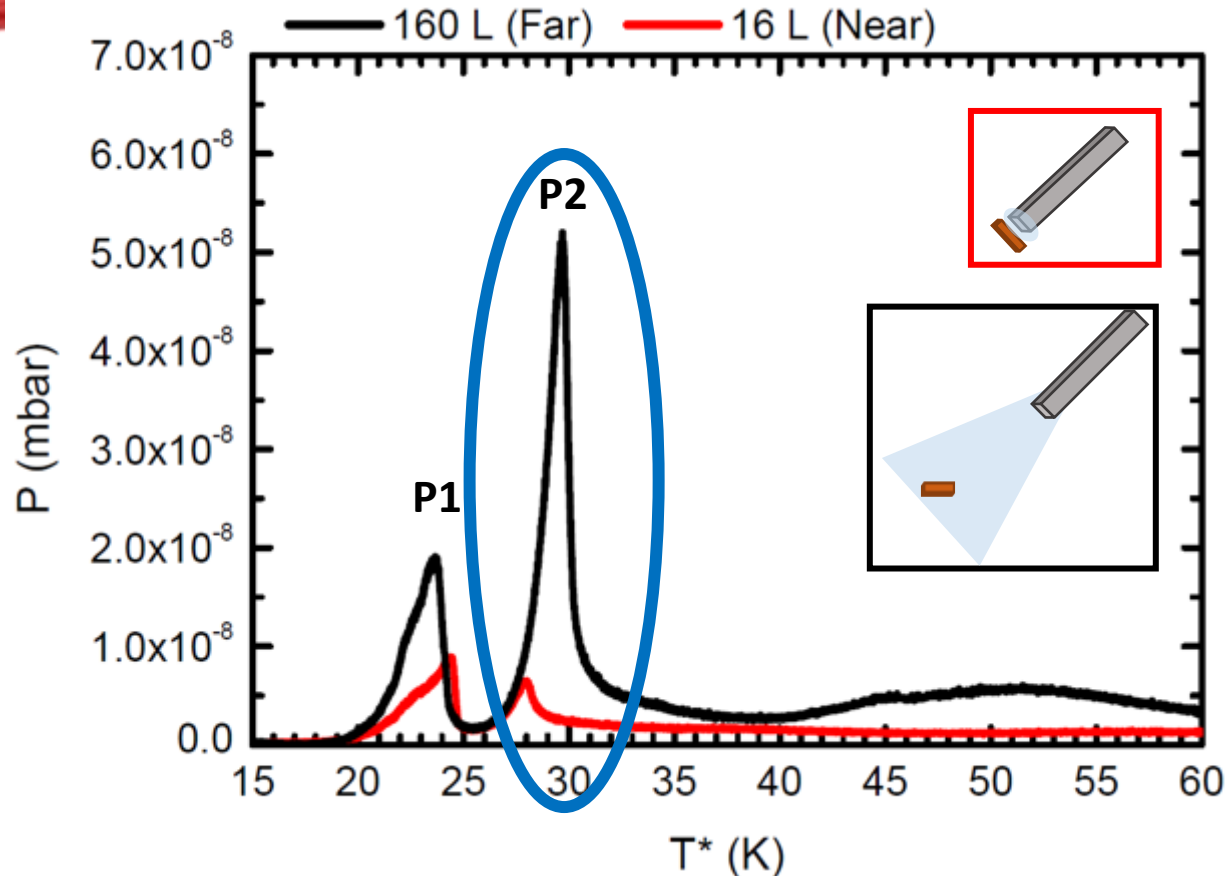
Near to the sample



$\approx 5-10$ Langmuir

Accurate Calibration in progress

Importance of dosing near the sample



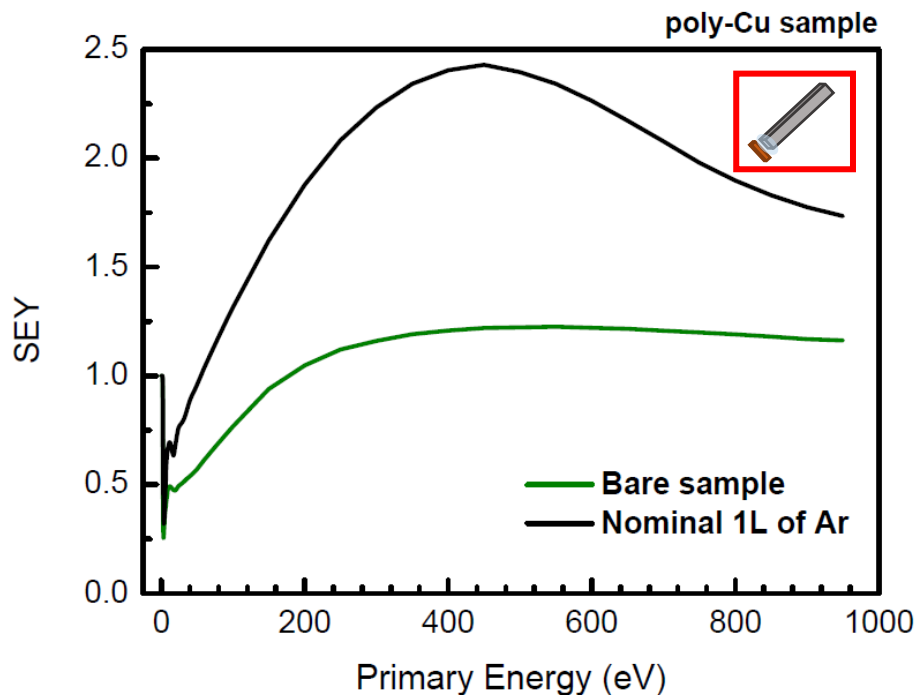
✓ Putting the doser near the sample is effective for the reduction of the desorption related to the manipulator

Coverage calibration by SEY

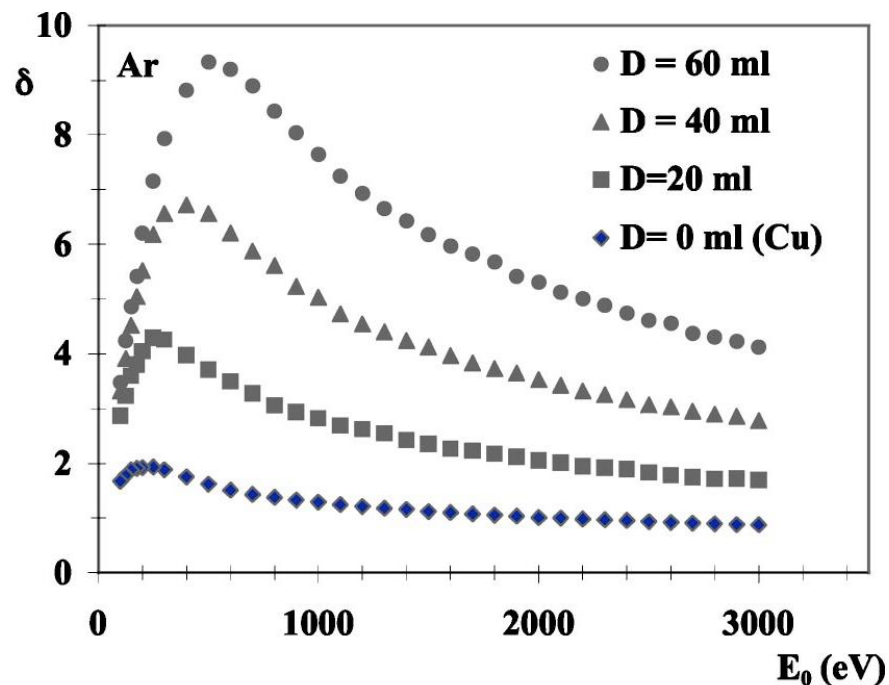
Accurate
Calibration in
progress



Coverage calibration by SEY

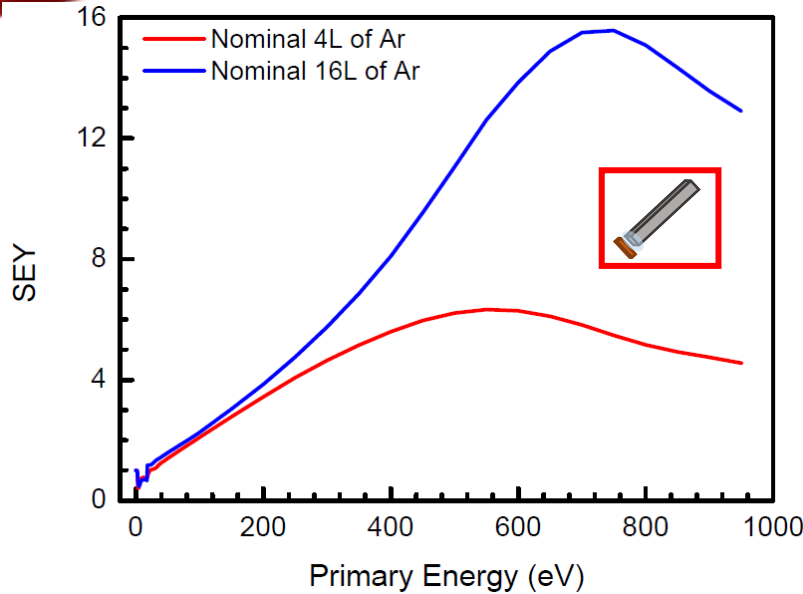


✓ Nominal 1L of Ar dosed in the vacuum chamber corresponds to a coverage of $\sim 10L$ on the sample surface



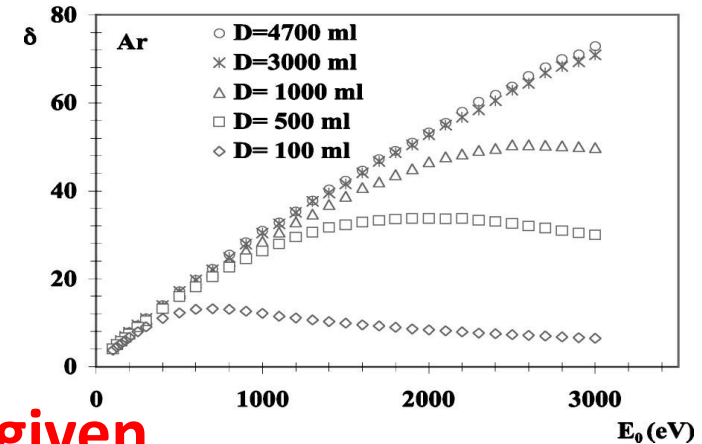
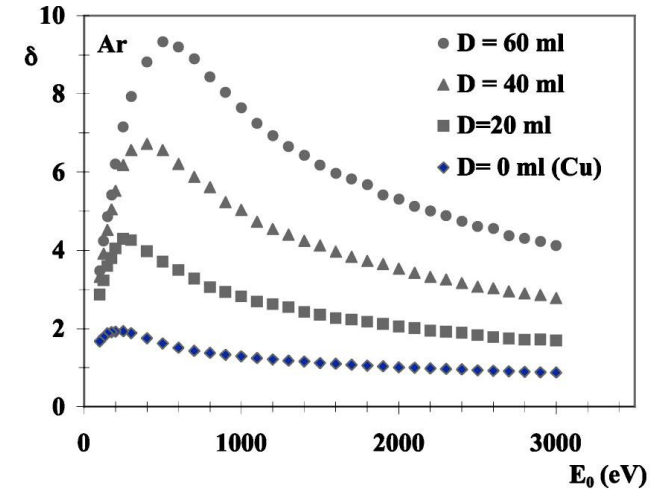
J. Cazaux et al.; Phys. Rev. B, 71 (2005)

Coverage calibration by SEY



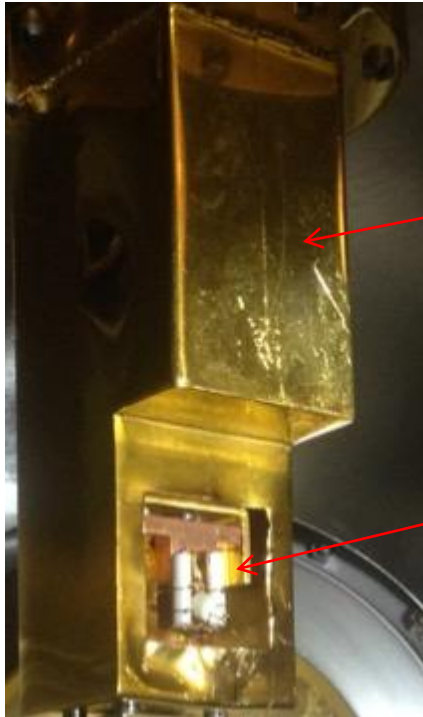
✓ Nominal 4L and 16L of Ar dosed in chamber correspond to a coverage of $\sim 25\text{L}$ and $\sim 100\text{L}$ on the sample surface

J. Cazaux et al.; Phys. Rev. B, 71 (2005)



From here on, calibrated coverages are given

LNF-Cryogenic Manipulator

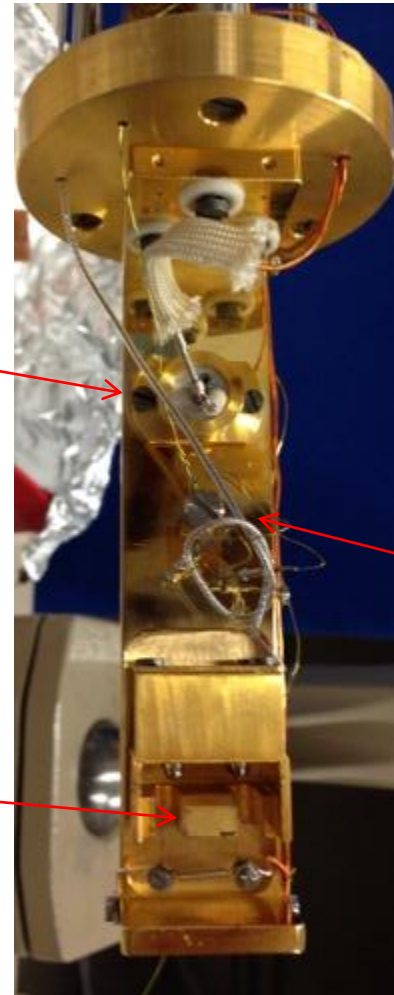


Screen

Sample

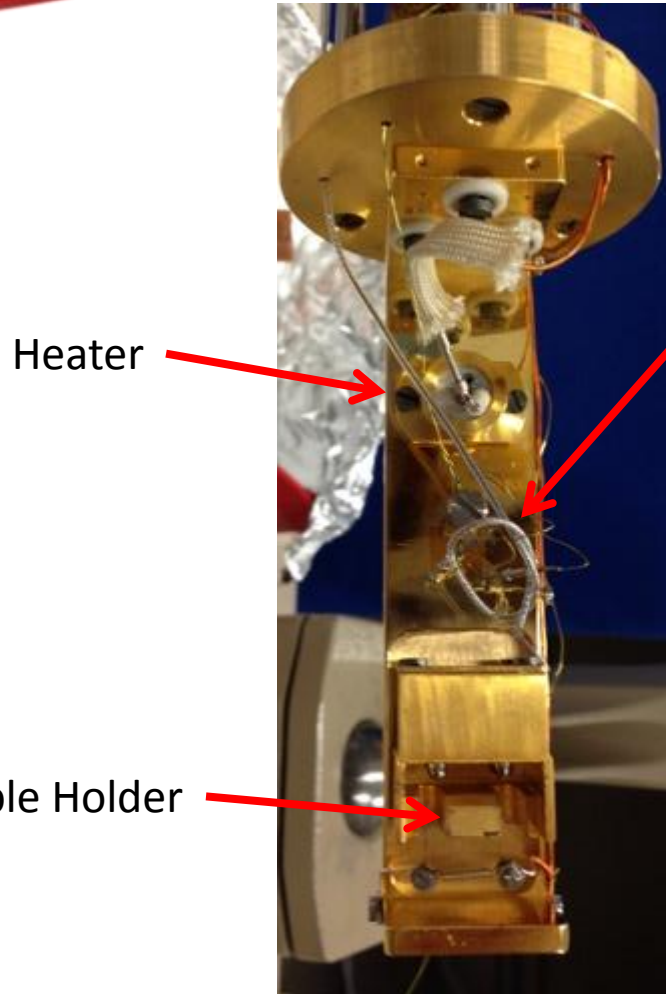
Heater

Sample Holder



Measured
Temperature

Temperature calibration

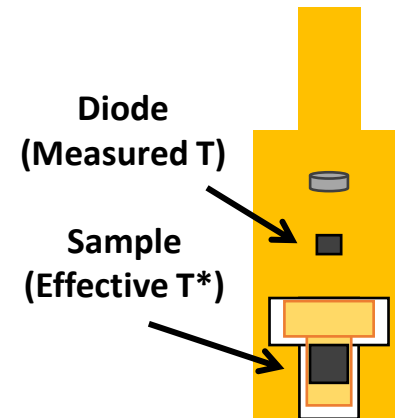


Measured
Temperature

Measured Temperature (T^*)

\neq

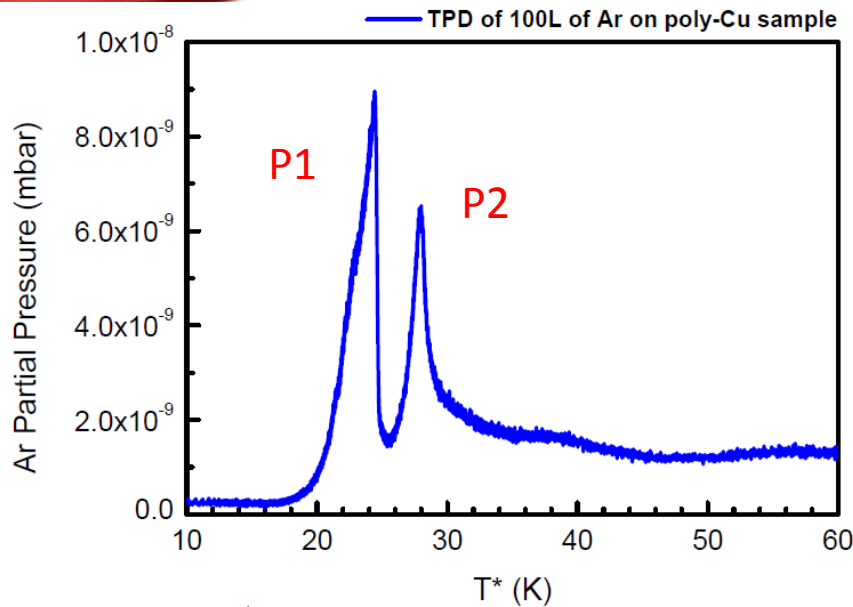
Sample Real Temperature (T)



Temperature calibration

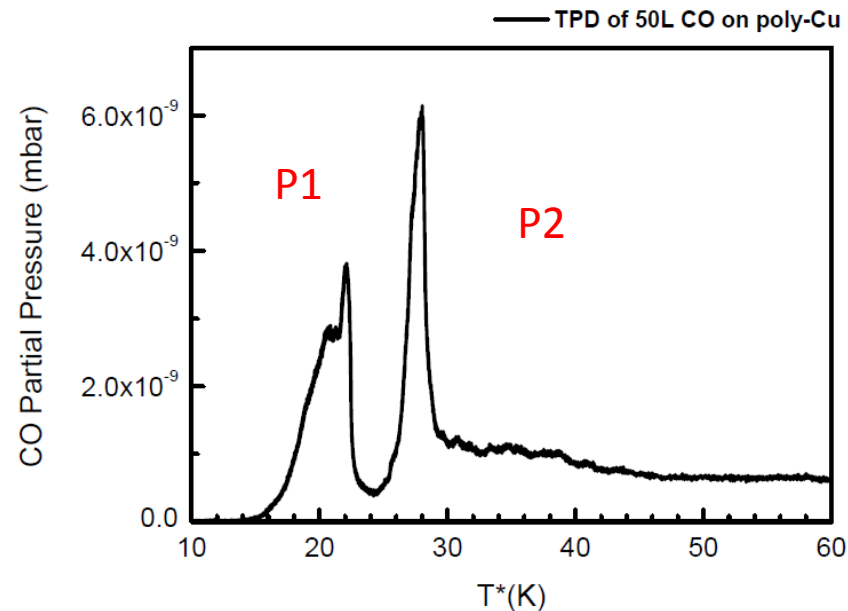
Temperature Programmed Desorption

The **different desorption peaks** are experimental artefact

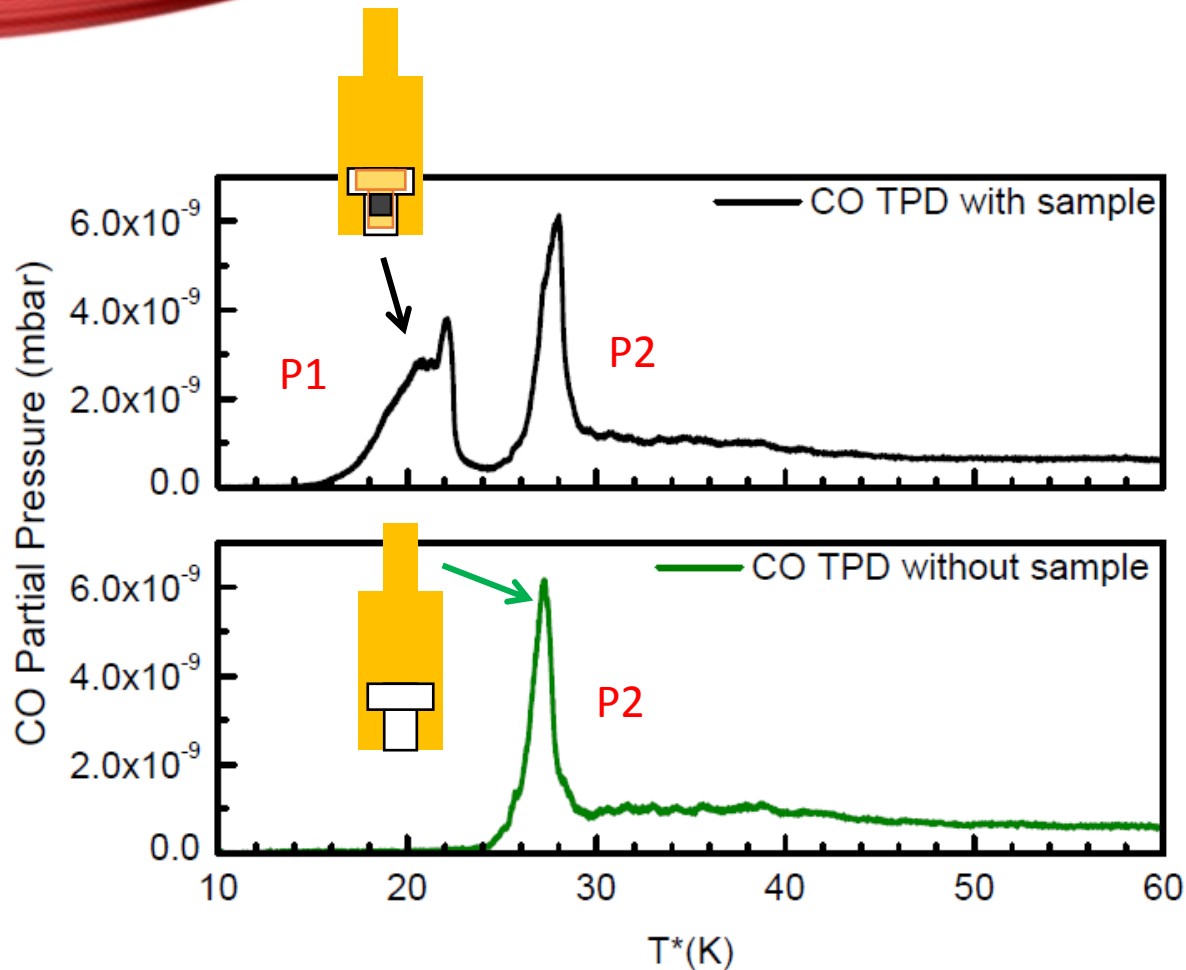


Example of as acquired Ar TPD curve

Example of as acquired CO TPD curve

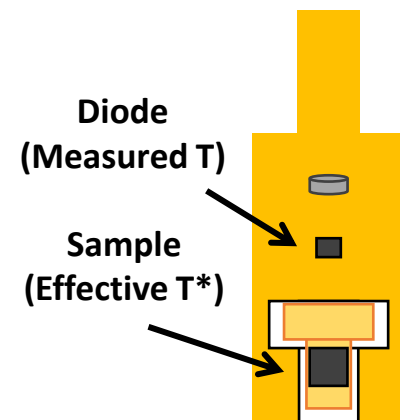


Temperature calibration



Peak 1: Desorption from sample ("hotter part" at T^*)

Peak 2: Desorption from Manipulator (at T)



Temperature calibration

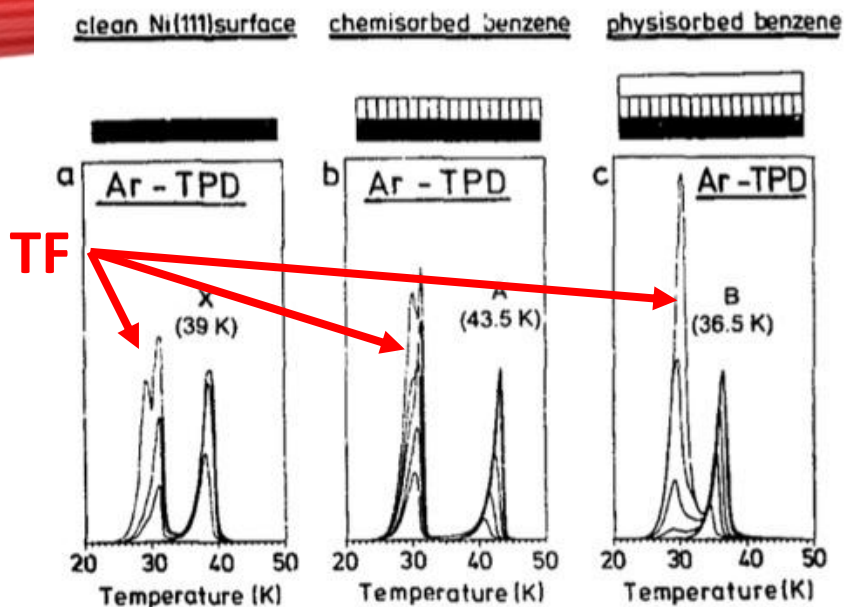


Fig. 1. Argon desorption spectra for increasing argon exposures onto various underlying "substrates": (a) clean Ni(111); (b) saturated chemisorbed ($\sqrt{7} \times \sqrt{7}$)R19.1° benzene layer on Ni(111); (c) saturated first physisorbed benzene layer on top of the chemisorbed layer. Adsorption temperature 22 K; heating rate 1 K/s. The "substrates" are schematically indicated above the corresponding TPD spectra.

M. Stichler et al.; Surface Science 348 (1996)

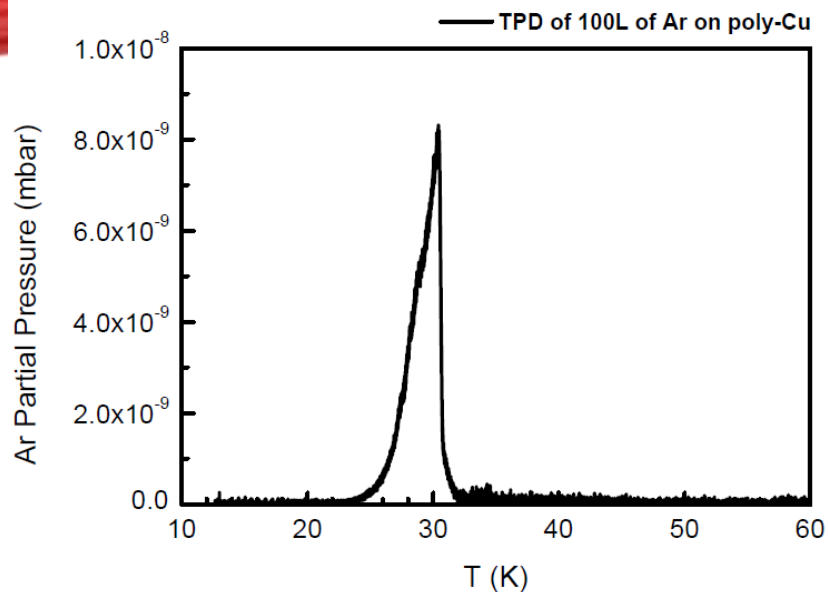
J. A. Noble et al., Mon. Not. R. Astron. Soc., 421 (2012)
R. S. Smith et al., J. Phys. Chem. B, 120 (2016)
T. Suhasaria et al., Mon. Not. R. Astron. Soc., 472 (2017)

Same Desorption temperature of Argon Thick Film (TF) on different substrates

Ar TF desorbs at a unique $T \sim 30$ K

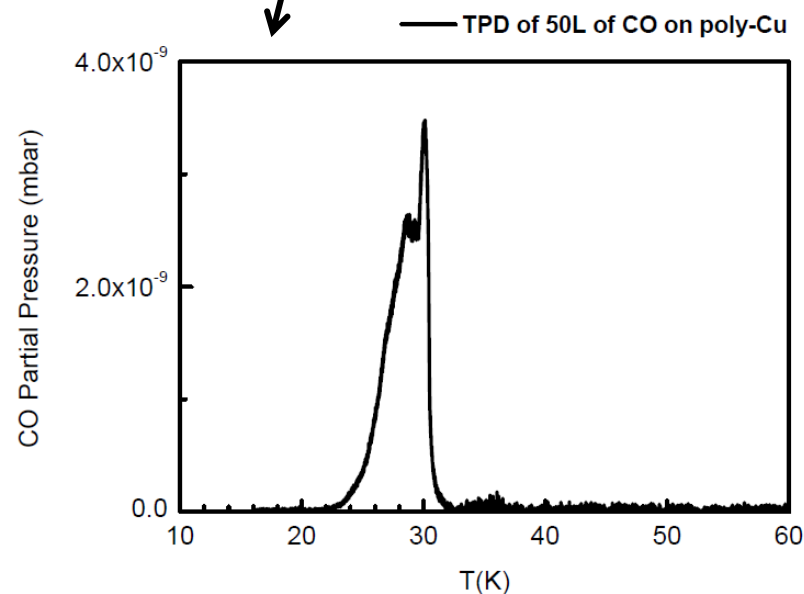
From literature, CO and CH₄TF desorb at $T \sim 30$ K a $T \sim 37$ K respectively

Temperature calibration

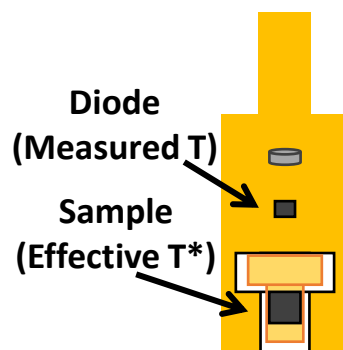


Example of Ar TPD curve after data analysis

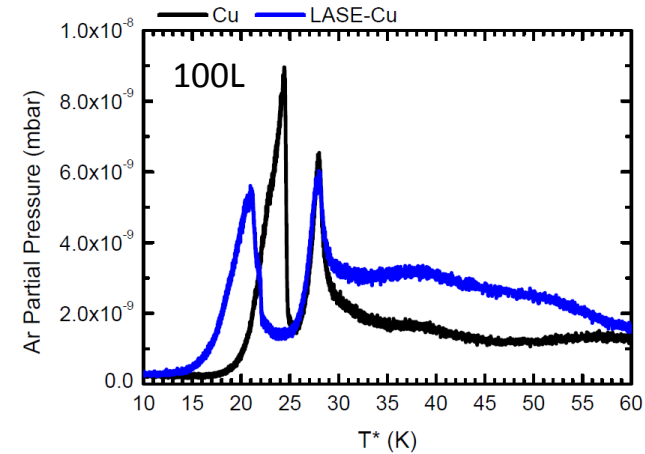
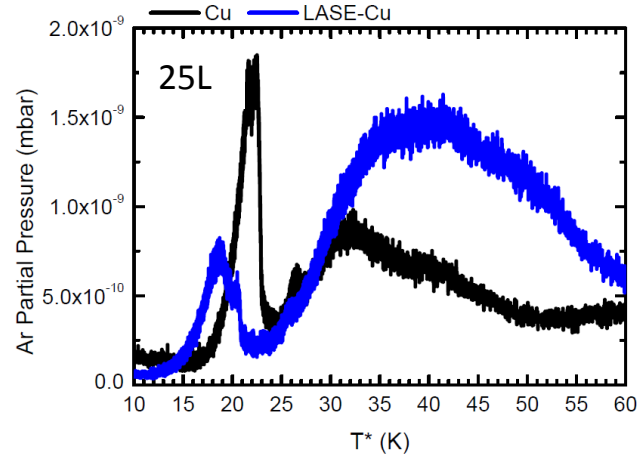
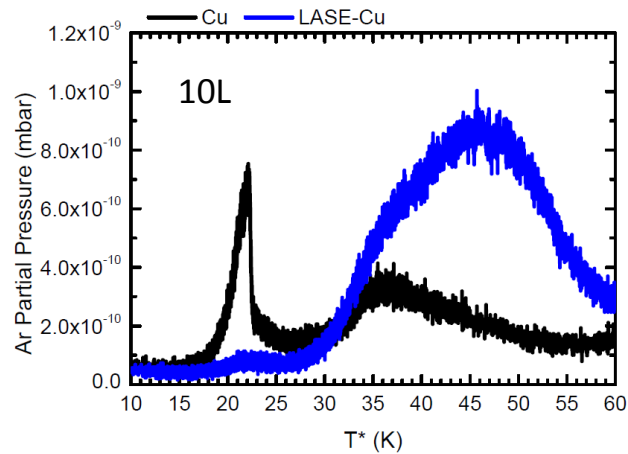
Example of CO TPD curve after data analysis



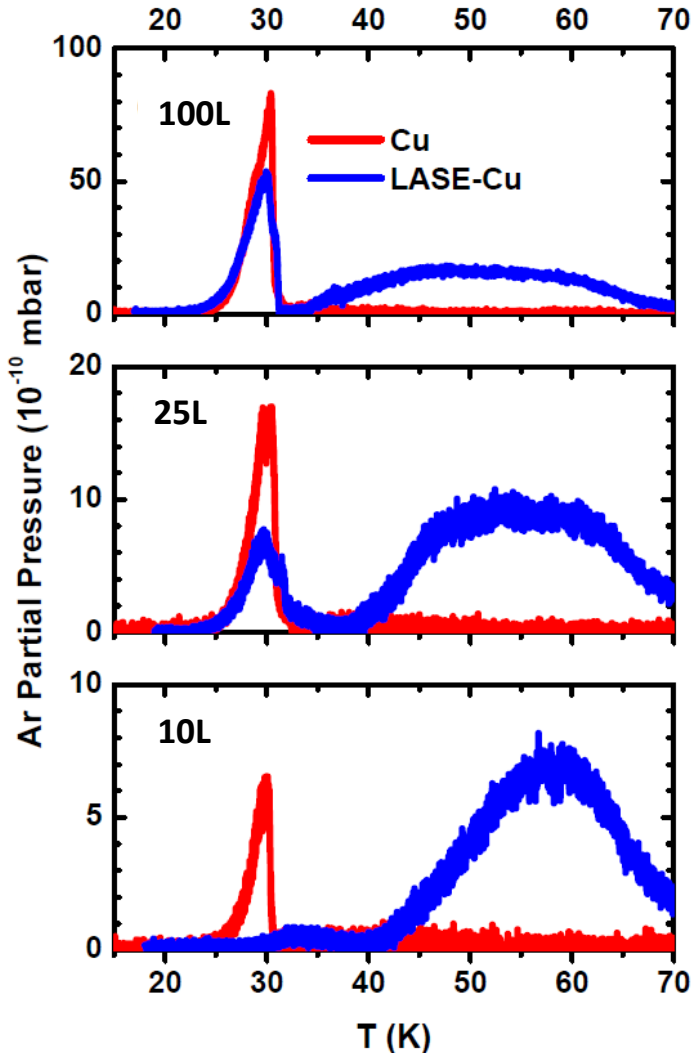
Temperature correction from T^* to real T



Synopsys of the raw data



Final Ar TPD results

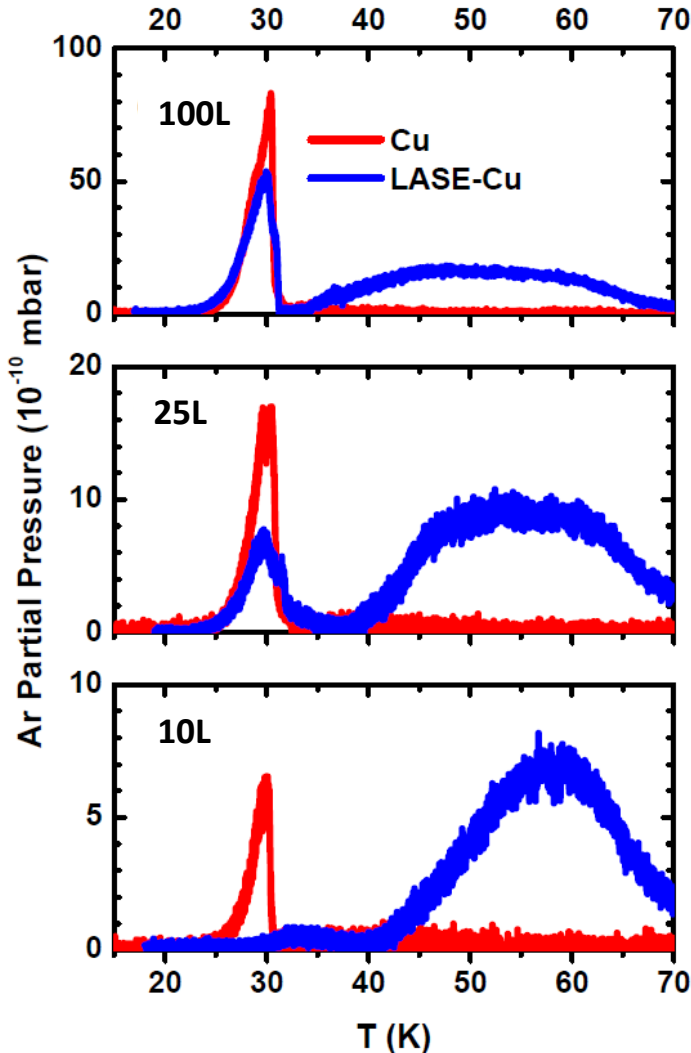


Poster presentation at the FCC Week 2018 and talk presentation at EuroCirCol Meeting in Amsterdam



Oral presentation at the e-Cloud 18 in Isola d'Elba

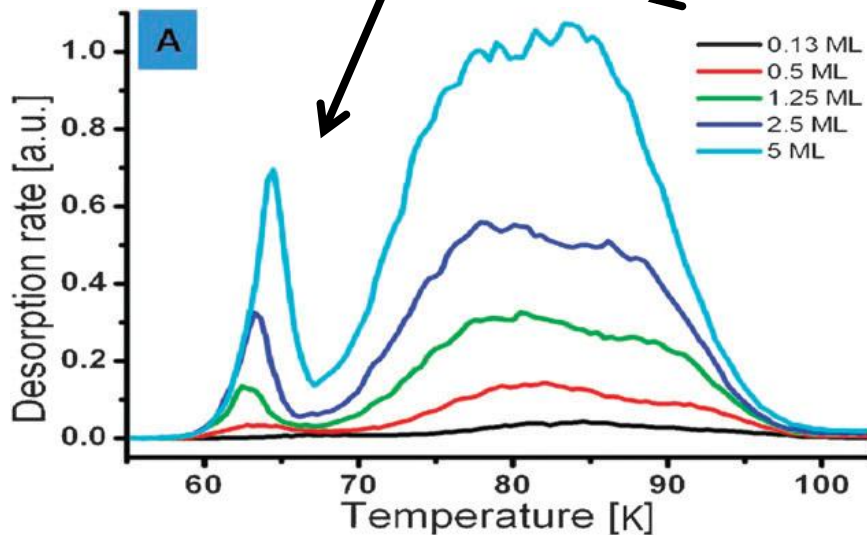
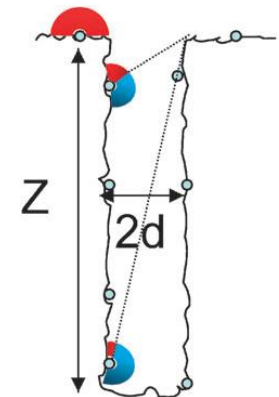
2 publications in preparation: one regular article and the e-Cloud 18 proceeding



- On flat Cu Ar adsorbs due to the weak Ar-Cu and Ar-Ar Van der Waals interactions and the desorption curve consists of the sharp peak at $T \sim 30$ K.
- For the LASE-Cu substrate the Ar adsorption energy at the undercoordinated surface defect sites increases and desorption occurs at higher T. However, at high coverage, multilayer desorption at $T \sim 30$ K is also observed.

Desorption from the top surface and from the topmost part of the pore

Desorption from pore depth



High temperature TPD peak

Due to the wide distribution of the binding energy of the adsorption sites and multiple desorption–readsorption cycles on the inner pore walls

PAPER

www.rsc.org/pccp | Physical Chemistry Chemical Physics

Xe interacting with porous silicon

Assaf Paldor,^a Gil Tokor,^a Yigal Lilach^b and Micha Asscher^a

Received 17th December 2009, Accepted 29th March 2010

First published as an Advance Article on the web 30th April 2010

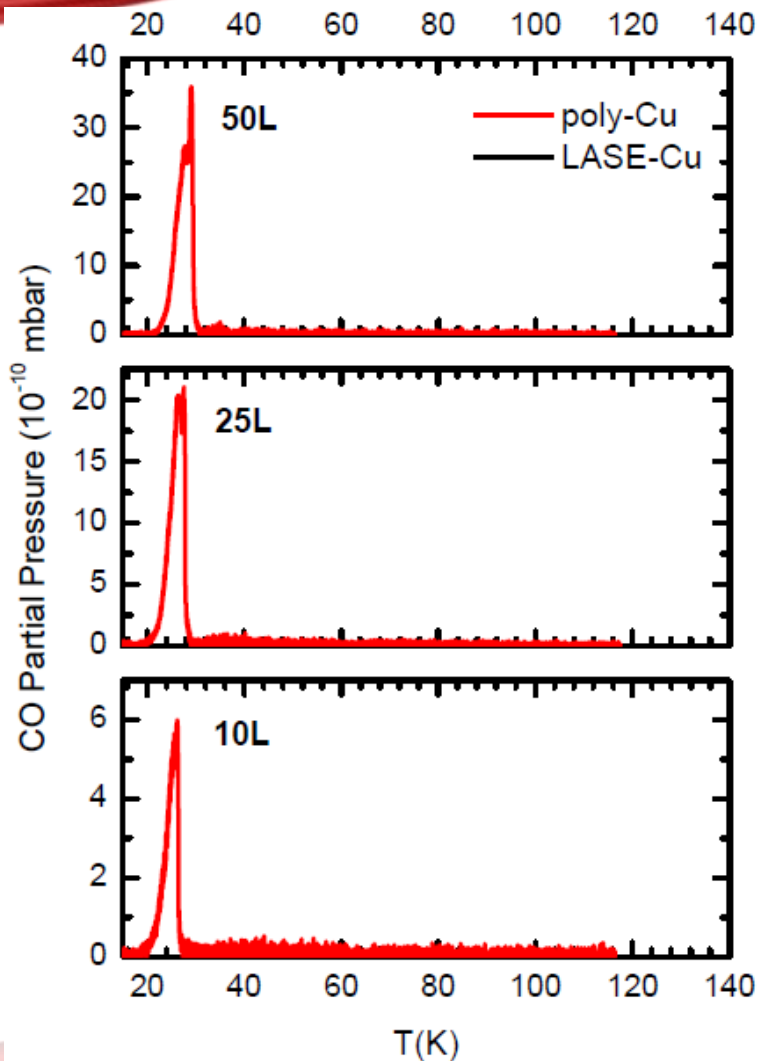
DOI: 10.1039/b926692e



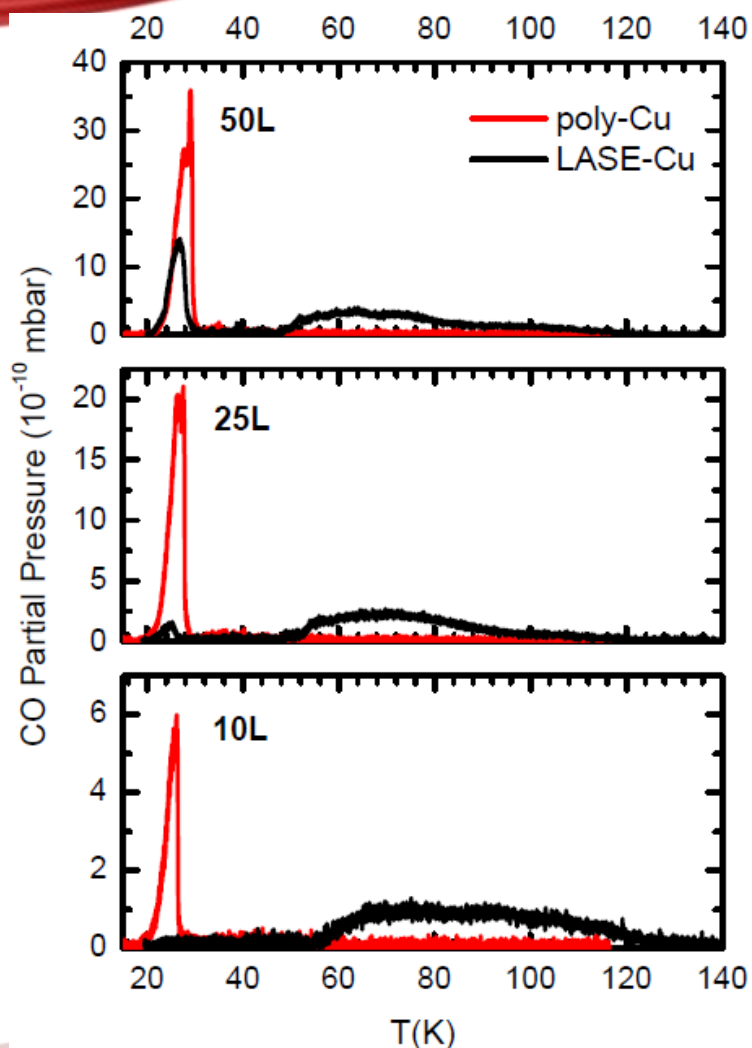
EuroCirCol Meeting in Karlsruhe

- ✓ Temperature calibration
- ✓ Coverage calibration

CO and CH₄ thermal desorption measurements: preliminary results

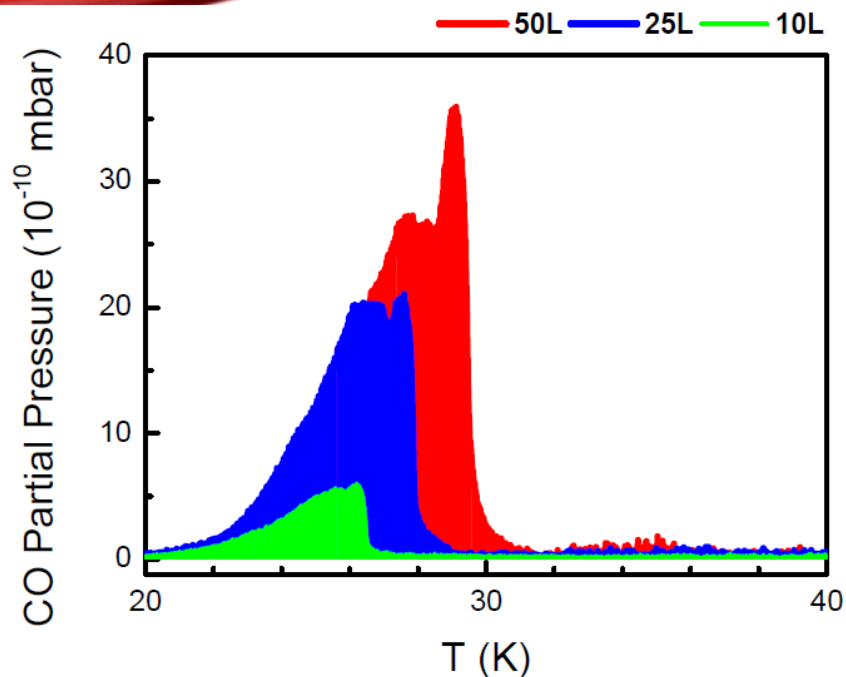


- On flat Cu CO adsorbs due to the weak CO-Cu and CO-CO Van der Waals interactions and the desorption curve consists of the sharp peak at $T \sim 30$ K.



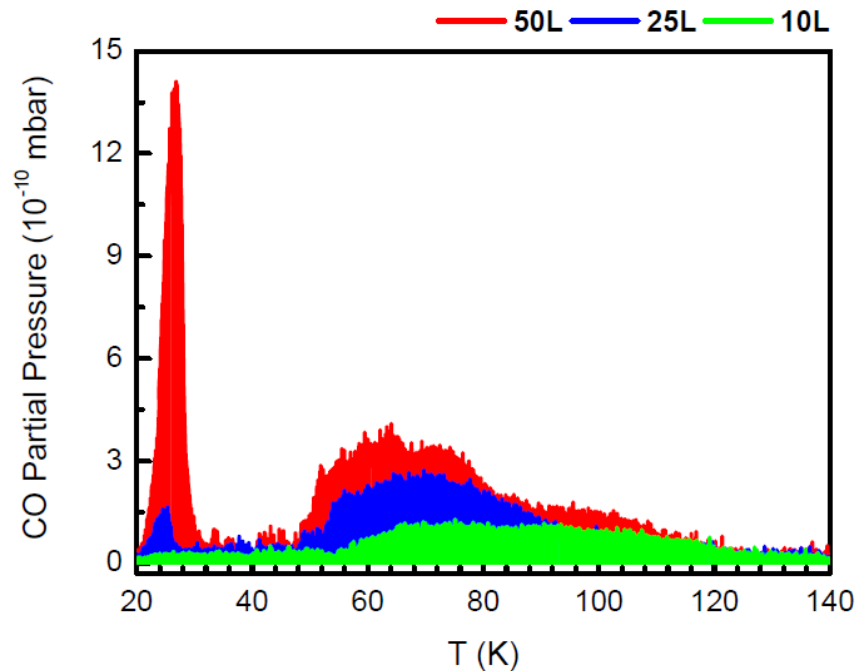
- On flat Cu CO adsorbs due to the weak CO-Cu and CO-CO Van der Waals interactions and the desorption curve consists of the sharp peak at $T \sim 30$ K.
- For the LASE-Cu substrate the CO adsorption energy at the undercoordinated surface defect sites increases and desorption occurs at higher T . However, at high coverage, multilayer desorption at $T \sim 30$ K is also observed.

CO TPD Measurements

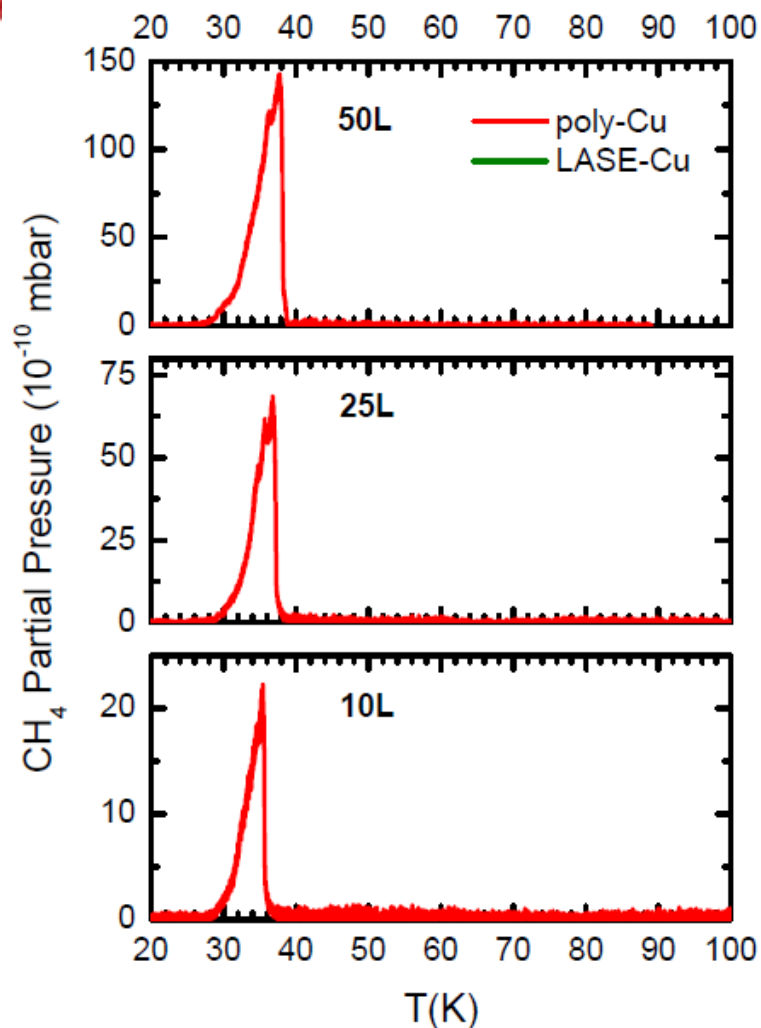


← CO TPD curve from poly-Cu

CO TPD curve from LASE-Cu →

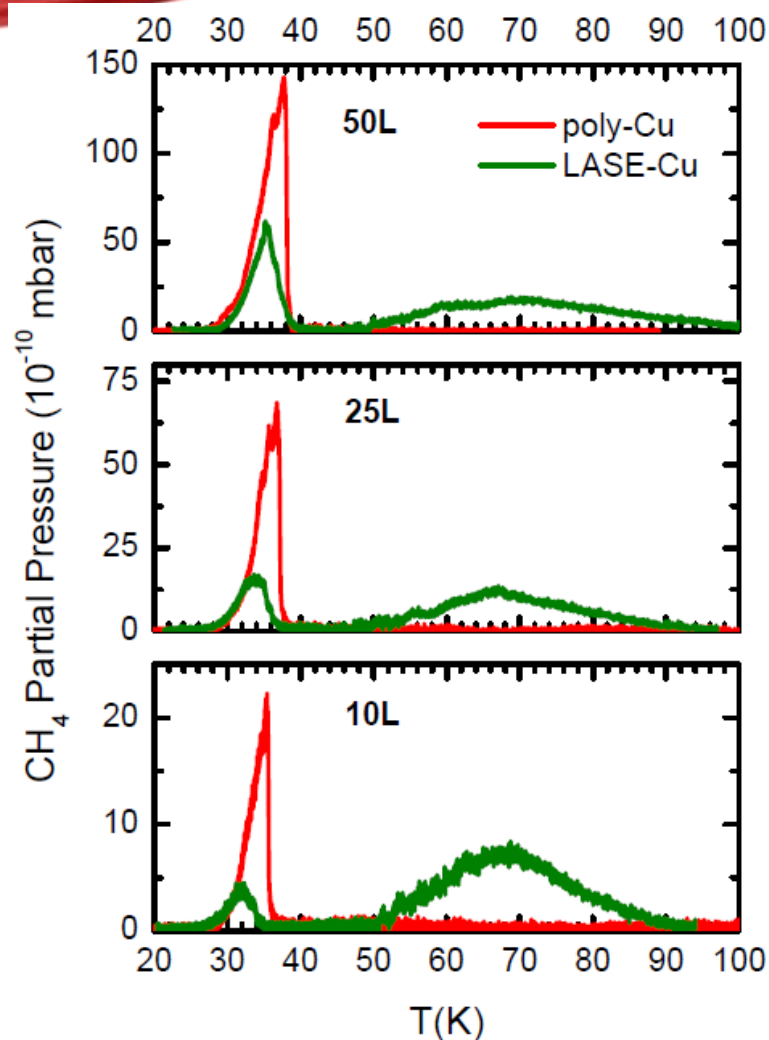


CH₄ TPD Measurements



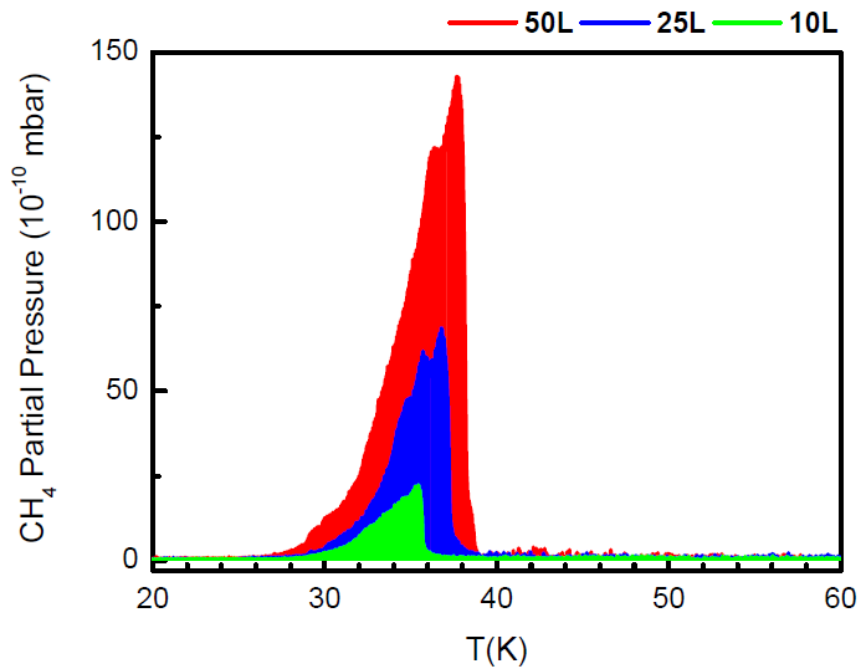
- On flat Cu CH₄ adsorbs due to the weak CH₄-Cu and CH₄-CH₄ Van der Waals interactions and the desorption curve consists of the sharp peak at T~39 K.

CH₄ TPD Measurements

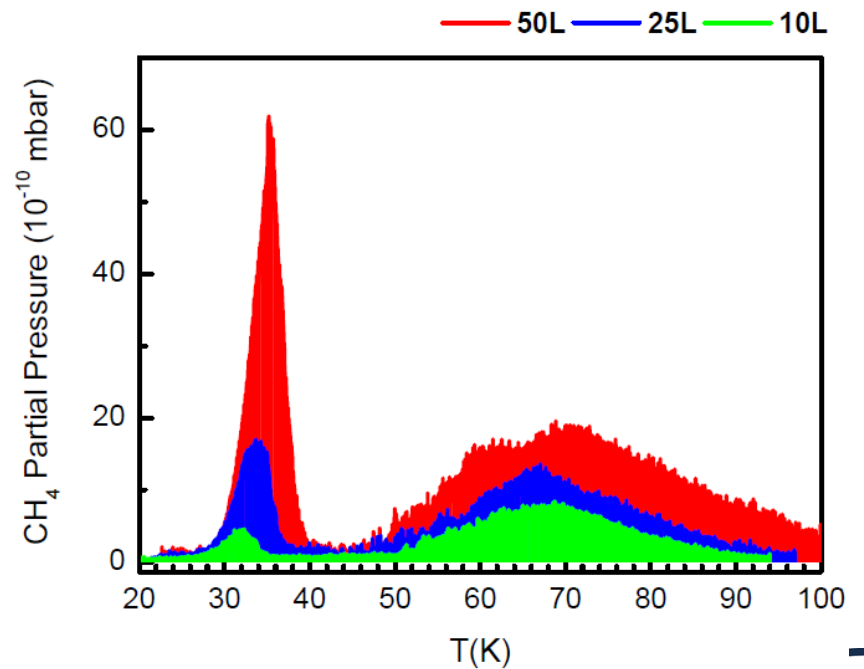


- On flat Cu CH₄ adsorbs due to the weak CH₄-Cu and CH₄-CH₄ Van der Waals interactions and the desorption curve consists of the sharp peak at T~39 K.
- For the LASE-Cu substrate the CH₄ adsorption energy at the undercoordinated surface defect sites increases and desorption occurs mainly at higher T. However, on increasing the coverage, the multilayer desorption at T~39 K also increases.

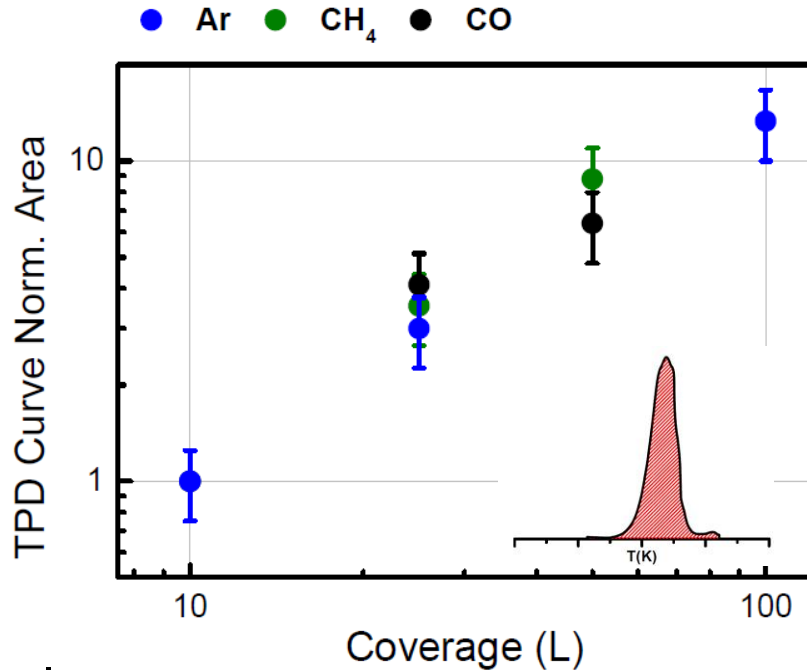
CH₄ TPD Measurements



CH₄ TPD curve from LASE-Cu



✓ The TPD results here reported confirm that what has been observed for Ar is a general trend common to some specific gases present as contaminant in accelerators

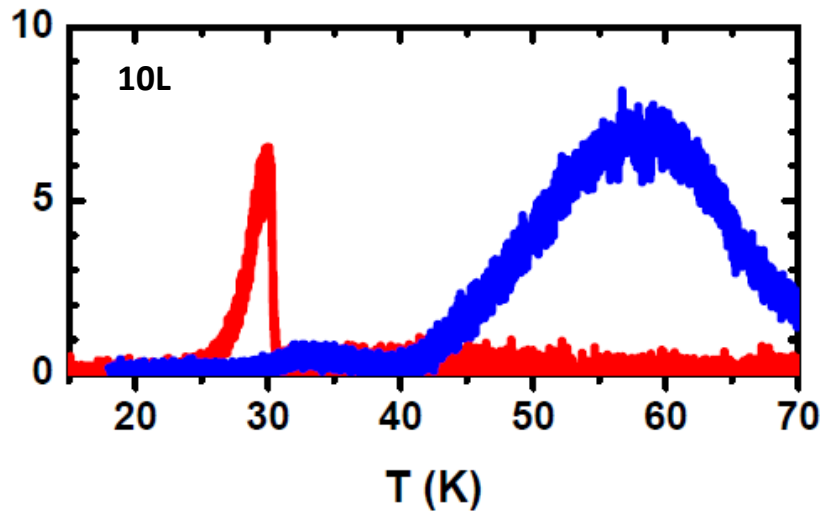


Gases dosed on poly-Cu substrate



→ Normalization to the TPD curve area at the lower coverage

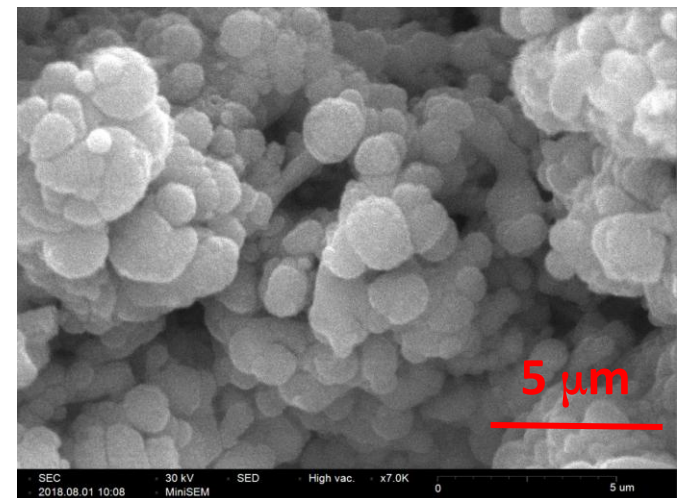
Ar TPD curve from poly-Cu and LASE-Cu



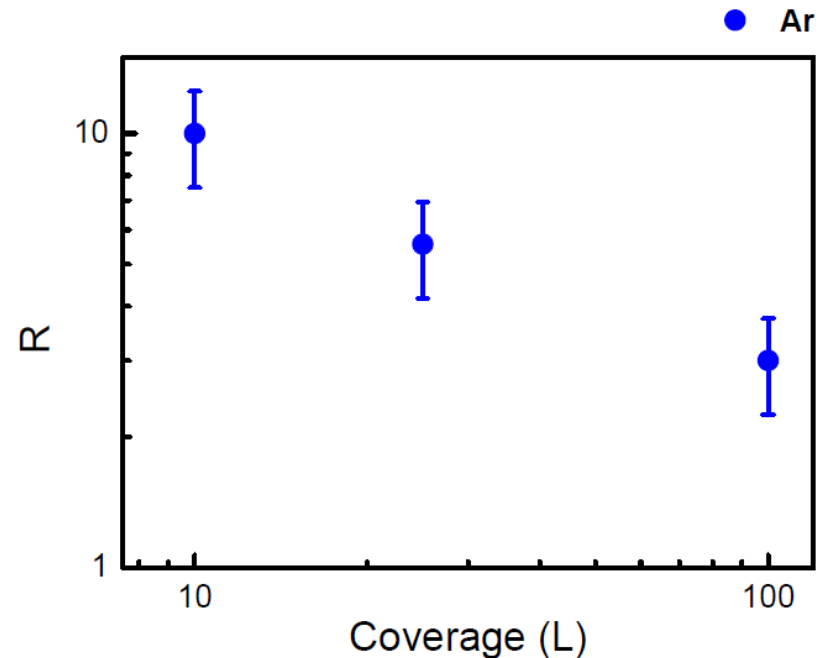
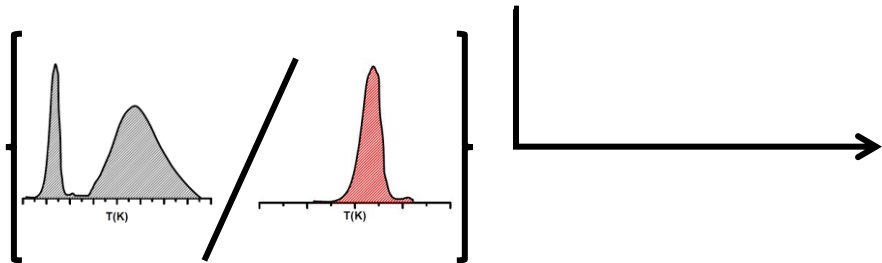
LASE-Cu can accommodate a larger quantity of gas so as expected by its morphology

Highly porous and inhomogeneous surface with nanometric features (undercoordinated surface defect sites)

Morphology of LASE-Cu by SEM
(G. Viviani @ LNF-INFN)



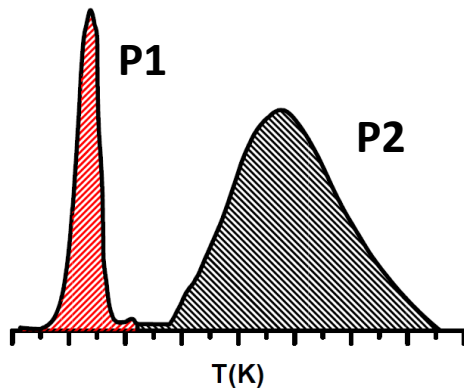
$$R = (\text{Ar on LASE-Cu TPD Curve Area}) / (\text{Ar on poly-Cu TPD Curve Area})$$



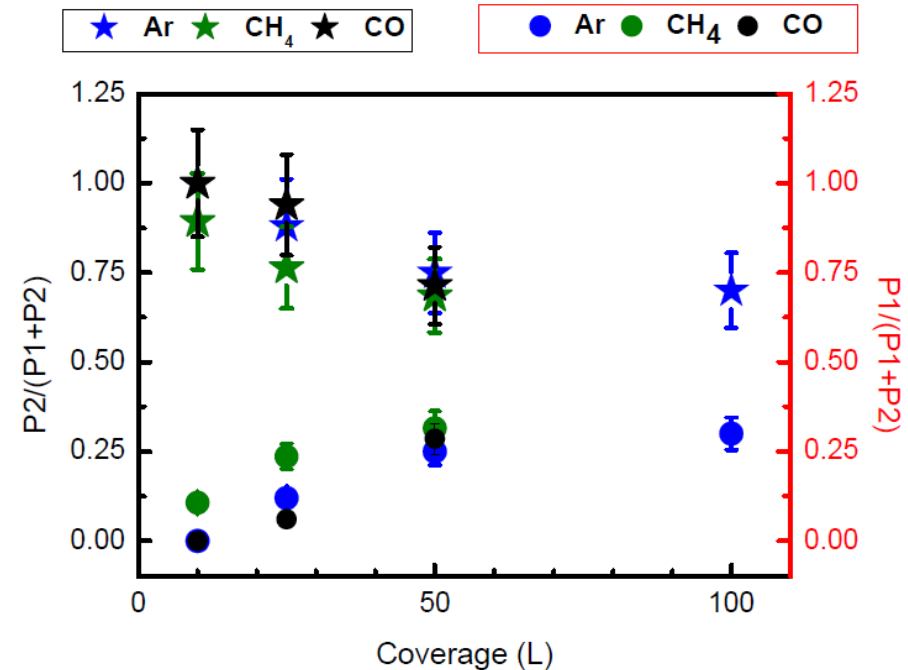
Accurate measurement of the specific surface is lacking. In this covering range, it's **at least about 10 times larger** than poly-Cu surface

This trend accounts for the desorption (and adsorption) kinetics of the gas in the LASE-Cu substrate determined by its morphology

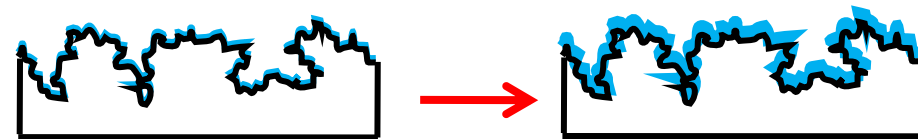
$$P2/(P1+P2) = (\text{TPD Curve Area under } P2) / (\text{Total TPD Curve Area})$$



Gas desorption kinetics on LASE-Cu

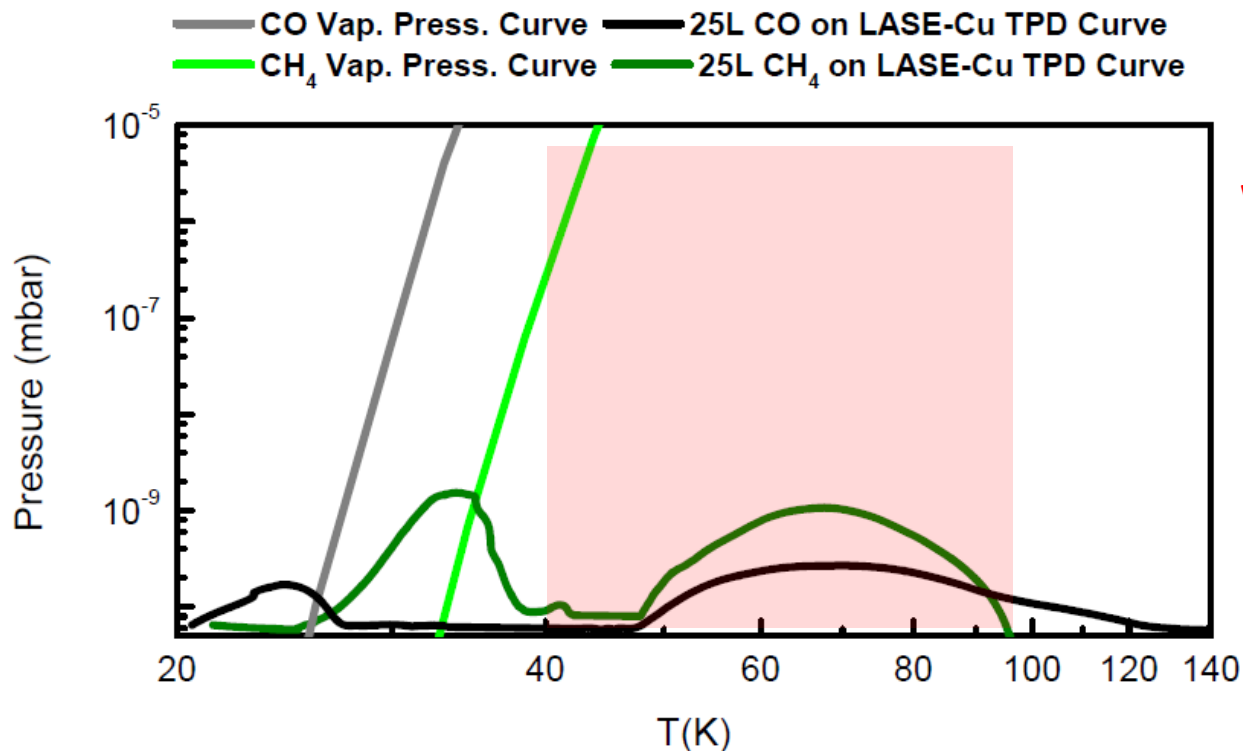


Ubiquitous P2 contribution spreading in a broad temperature range



Gradually occupation of all available adsorption sites (pores wall included), up to saturation and ice thickening also on top surface

Saturated vapour pressure from Honig and Hook (1960)



Wide desorption contribution over 40 K due to the morphological structuring of the material (intrinsic broad distribution of adsorbing defective sites and pores)

WARNING!

This could render very difficult to find a temperature interval for the LASE-type sample here studied where vacuum stability could be granted for all the molecular species composing the residual gas in the beam pipe components

Conclusion

- The use of this type of LASE-substrate could be a problem for vacuum stability issues



Outlook

- Electron and photo-desorption investigations
- Better estimate of the consequences of such distributed temperature desorption via gas dynamic studies in real machines
- Optimization of LASE and SEY mitigation studies to optimize a material which is compliant both for SEY reduction and for vacuum stability
 - Improve synergies between the different studies
 - Long work: to be performed during EURO-CIRCOL2?



E. La Francesca R. Cimino R. Larciprete
M. Angelucci A. Liedl L. Spallino

The low temperature team at LNF



DAΦNE-L Team:
M. Pietropaoli and G. Viviani



A SUPPORTING PROJECT FUNDED BY INFN-SNC5